ETHZ-IPP PR-98-04
13 July 1998

Letter-of-Intent for a Precision Measurement of the μ^+ Lifetime (G_F) with the FAST detector

F. Navarria, G. Valenti
Univ. Bologna, Bologna, Italy

P. De Jong, F. Filthaut, J. Kirkby[1)], L. Malgeri, G. Passaleva, C. Tully
CERN, Geneva, Switzerland

H. Anderhub, R. Nahnhauer[2)], M. Pohl, S. Waldmeier, R. Wetter
ETH, Zurich, Switzerland

K. Deiters, F. Foroughi, C. Petitjean, D. Renker
PSI, Villigen, Switzerland

T. Case, K. Crowe, P. Kammel
UCB and LBNL, Berkeley, USA

Abstract

We propose to measure the μ^+ lifetime to a precision of 2 ps with the fibre active scintillator target, FAST. This represents a factor 20 improvement beyond the present world experimental average. After including the theory error and the muon mass error, 3.2×10^{-7}, this will determine the Fermi coupling constant, G_F, to a precision of 10^{-6}, which also represents a factor 20 improvement. The experiment involves a small active target of dimensions about $20 \times 20 \times 20$ cm^3 made from scintillating plastic fibres viewed by position-sensitive phototubes. In order to control and reduce the systematic errors, it is proposed to perform the experiment with the same detector in two different beams. In the first stage, the measurement would be performed with a DC π^+ beam at 160 MeV/c and, in the second stage, with a time-structured π^+ beam at 106 MeV/c. The detector is designed to operate at an average beam rate of 1 MHz. Data samples of 10^{12} stopped π^+ events are required, corresponding to beam times between 14 days at 100% duty cycle and 140 days at 10% duty cycle.

[1)] contact person
[2)] Permanent address, DESY-Zeuthen, Germany

Contents

1 Physics motivation

In its electroweak sector, the Standard Model predicts tree level relationships among the couplings of the electromagnetic interaction, and the weak charged and neutral currents. This reduces the three couplings to two universal constants, conveniently chosen as the electric charge e and the weak mixing angle $\sin^2\theta_W$. One can view these as being defined by the trilinear couplings at the γW^+W^- and ZW^+W^- vertices; all matter couplings are then fixed. Moreover, the Higgs mechanism relates the weak mixing angle to the ratio of the masses of the intermediate vector bosons, m_W and m_Z. To test all these relationships with a set of precision measurements constitutes a complete test of the foundations of the Standard Model; and any deviations might hint of new directions beyond the Standard Model.

At LEP, SLC and the Tevatron, impressive progress has been made over the last few years on this large programme of precision measurements [1, 2]. A summary of the current experimental status is shown in Table 1, including the results of low energy measurements of α evolved to $q^2 = m_Z^2$ [3]. These data have experimentally verified the existence of weak radiative corrections, $\Delta r = f(\Delta\alpha, m_t, m_H)$, by confirming the fundamental relationship

$$G_F = \frac{\pi\alpha}{\sqrt{2}} \cdot \frac{m_Z^2}{m_W^2\,(m_Z^2 - m_W^2)} \cdot \frac{1}{1-\Delta r}\,.$$

The weak radiative corrections provide indirect measurements of the masses of the top quark and the Higgs boson, with precisions limited by the experimental errors on the fundamental parameters. This determination of the top quark mass is in good agreement with the direct measurements at the Tevatron.

Table 1: Present experimental precision of fundamental parameters of the Standard Model [1, 2].

Quantity	Symbol	Value (error)	Precision (ppm)
Fermi coupling constant	G_F	1.166 39 (2) $\times 10^{-5}$ GeV^2	20 ($\stackrel{\text{FAST}}{\longrightarrow}$ 1)
Weak mixing angle	$\sin^2\theta_{\text{eff}}^{\text{lept}}$	0.231 49 (21)	910
Fine-structure constant	$\alpha\,(m_Z^2)$	1/128.896 (90)	700
	$\alpha\,(0)$	1/137.035 989 5 (61)	0.045
W boson mass	m_W	80.375 (64) GeV/c^2	800
Z boson mass	m_Z	91.186 7 (20) GeV/c^2	22

The Fermi coupling constant has traditionally been one of the most precisely known among the electroweak parameters. While there has been no experimental progress in its value for the last 14 years, substantial advances have been made in the other parameters. For example, LEP has now reached a comparable precision for the Z mass (Table 1).

A factor 4 improvement in the W mass is expected at LEP 200 and the Tevatron, and further improvements are expected at future e^+e^- linear colliders. Experimental [4] and theoretical [5] progress is also expected on the precision of the fine structure constant evaluated at the electroweak scale. Despite these improvements, G_F will remain one of the most precisely known parameters in the Standard Model. Nevertheless, in view of its fundamental importance it should be measured with the highest possible experimental precision.

The experimental value of the Fermi coupling constant is determined from the measurement of the μ^+ lifetime, through the relationship,

$$\Gamma_\mu = \frac{1}{\tau_\mu} = \frac{G_F^2\, m_\mu^5}{192\,\pi^3} \cdot f(x) \cdot (1+\delta)\,,$$

where $f(x) = f(m_e^2/m_\mu^2)$ is an exactly-known phase space factor and δ represents radiative corrections which, until recently, have been known at the one-loop level. Theoretical uncertainties of higher-order radiative corrections contribute about half the present total error on G_F. The results of new calculations at the two-loop level are expected in the near future [6], and should effectively eliminate this source of error. The experimental precision of the μ^+ lifetime, which is the source of the other half of the present uncertainty in G_F, is dominated by three experiments that were completed 14–24 years ago, each with statistics of about 10^9 stopped μ^+ events:[3)]

τ_{μ^+} =	2197.110 ± 0.080	ns	M.P. Balandin et al. [7]
	2197.078 ± 0.073	ns	G. Bardin et al. [8]
	2196.950 ± 0.060	ns	K.L. Giovanetti et al. [9]
	2197.030 ± 0.040	ns	PDG96 [2] (1.8×10^{-5} precision)

We propose to measure the μ^+ lifetime to a precision of 2 ps [10] with the fibre active scintillator target detector, FAST. After including the muon mass error (3.2×10^{-7}) and the anticipated theoretical error in the radiative corrections, this will measure G_F to a precision of 10^{-6}, which is a factor 20 improvement of the present world average. The experiment requires a data sample of 10^{12} events and careful control of systematic errors.

In the same experiment we will also improve, by a factor 20, the measurement of the π^+ lifetime, which is presently

$$\tau_{\pi^+} = 26.033 \pm 0.005 \text{ ns} \qquad \text{PDG96 [2] } (1.9 \times 10^{-4} \text{ precision})$$

The π^+ lifetime measures the product of the pion decay constant and the CKM matrix element: $f_\pi^2\,|V_{ud}|^2$. We propose to measure τ_{π^+} to a precision of 10^{-5}.

2 Detector design

2.1 Detector concept

A precision determination of the μ^+ lifetime requires a measurement over a period of about 10 τ_{μ^+}, i.e ~ 20 μs. Previous experiments with DC beams could accept only a single muon

[3)] It is interesting to note that the experiments on the anomalous muon magnetic moment, $(g-2)_\mu$, in storage rings are unable to improve the precision of the muon lifetime because of uncertainties in the beam energy (Lorentz factor).

during this period and so were limited to beam rates below 20–50 kHz. Where pulsed beams were used, rate effects limited the useful intensities even more.

The concept of FAST (Figs. 1 and 2) is to construct a fast and highly granular detector that effectively performs 20 or more individual muon measurements *in parallel* at any given time. A π^+ beam is ranged out inside an active target that can image, measure and record events at a very high rate of 1 MHz. Two different detector geometries are being evaluated in a study of the systematic errors: a "block" geometry (Fig. 1), and a "card-deck" geometry (Fig. 2).

In the first stage of the experiment, the detector would be operated in a DC π^+ beam. Here the detector is designed to a) observe each individual stopping π^+ and measure its arrival time, b) detect the decay $\pi^+ \rightarrow \mu^+\nu_e$ and measure its time and stop location, c) watch that location for 20 μs and measure the time of the $\mu^+ \rightarrow e^+\nu_e\bar{\nu}_\mu$ decay, and d) reject the μ^+ if a second muon overlaps the stop fiducial region during the pre-defined sensitive time ($\pm$20 μs).

In the second stage of the experiment, the detector would be operated with a time-structured π^+ beam. Here a pulse of several tens of beam particles are injected into the target in a short time interval, and then the beam is switched off for about 20 μs. This effectively creates a small "radioactive" muon source inside the detector which decays over this period. The time of each individual muon decay in a given pulse is recorded relative to a common start time.

For both types of operation a highly granular detector that can handle very high event rates is required. The detector must also be 100% efficient for minimum ionizing tracks over the full solid angle. Performing the experiment with the same apparatus under two different beam conditions will provide two measurements of the μ^+ lifetime with quite different systematic errors. This will provide a powerful technique for understanding and reducing the overall systematic error of the final measurement (see Section 4).

The active target is essentially an extremely fast electronic imaging detector that emphasises speed, timing and pulse height measurements of charged particles, albeit with modest (~1 mm) position resolution. The detector relies on several technologies that have enjoyed dramatic progress over the last few years:

1. Plastic scintillating fibres (SCIFI).

2. Position-sensitive (multi-anode) photomultiplier tubes (PSPM).

3. Fast, pipelined (dead-timeless) front-end electronics.

4. Massive on-line computing capacity—data bandwidth, processing power and data storage capacity—which allows data to be collected and analysed in real-time at very high rates, and allows the recording of huge data volumes.

These are discussed in more detail below.

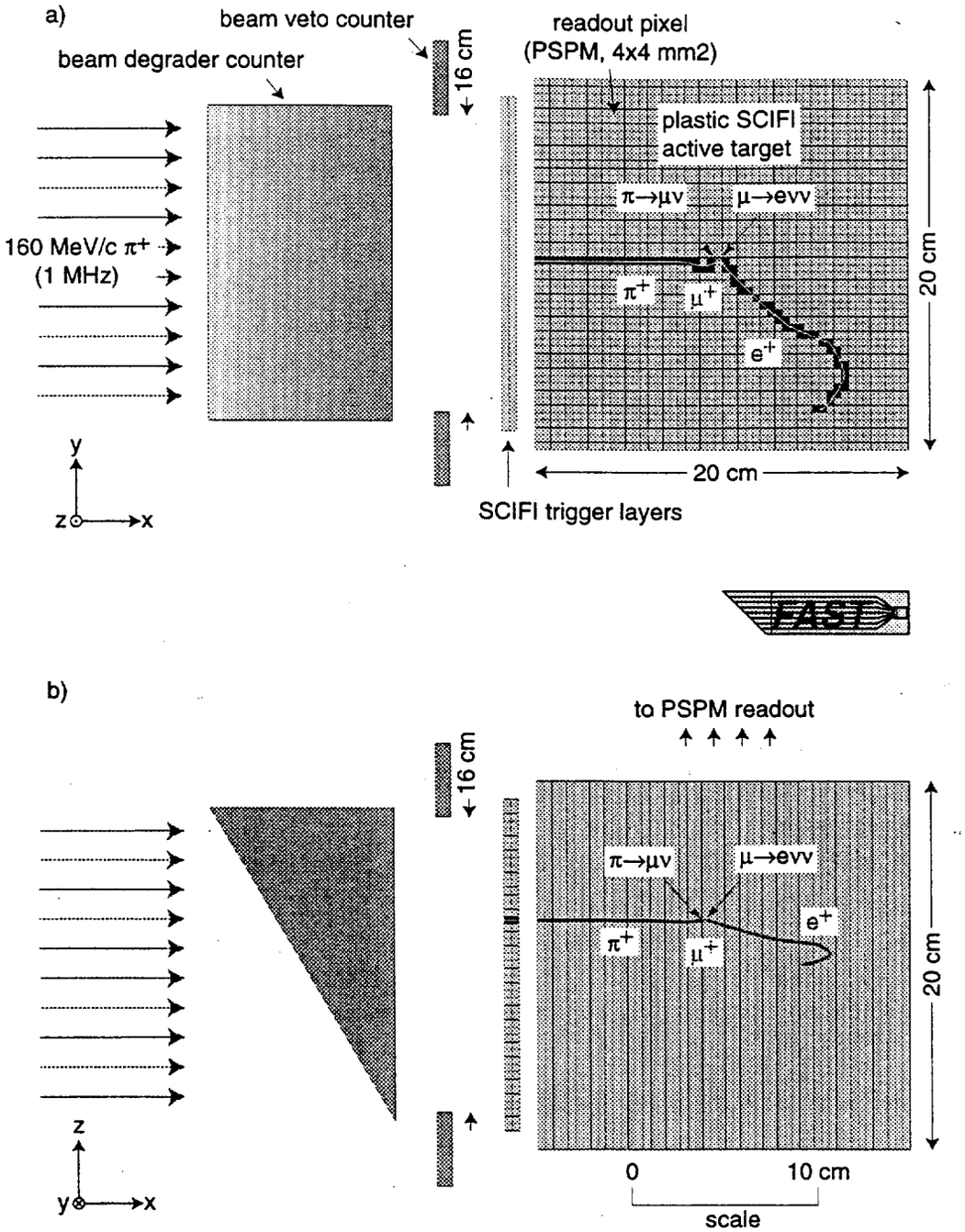

Figure 1: Option I for the FAST detector with a "block" geometry: a) xy projection and b) xz projection. Each of the small squares corresponds to one readout pixel (with a signal of 25 p.e./mip). The stopping points of the beam are spread over an area of about 16×16 cm^2 in the xy projection. The spread in the depth (x) coordinate is achieved by a combination of the effects of straggling, beam energy spread and the wedge-shaped counter at the entrance of the detector.

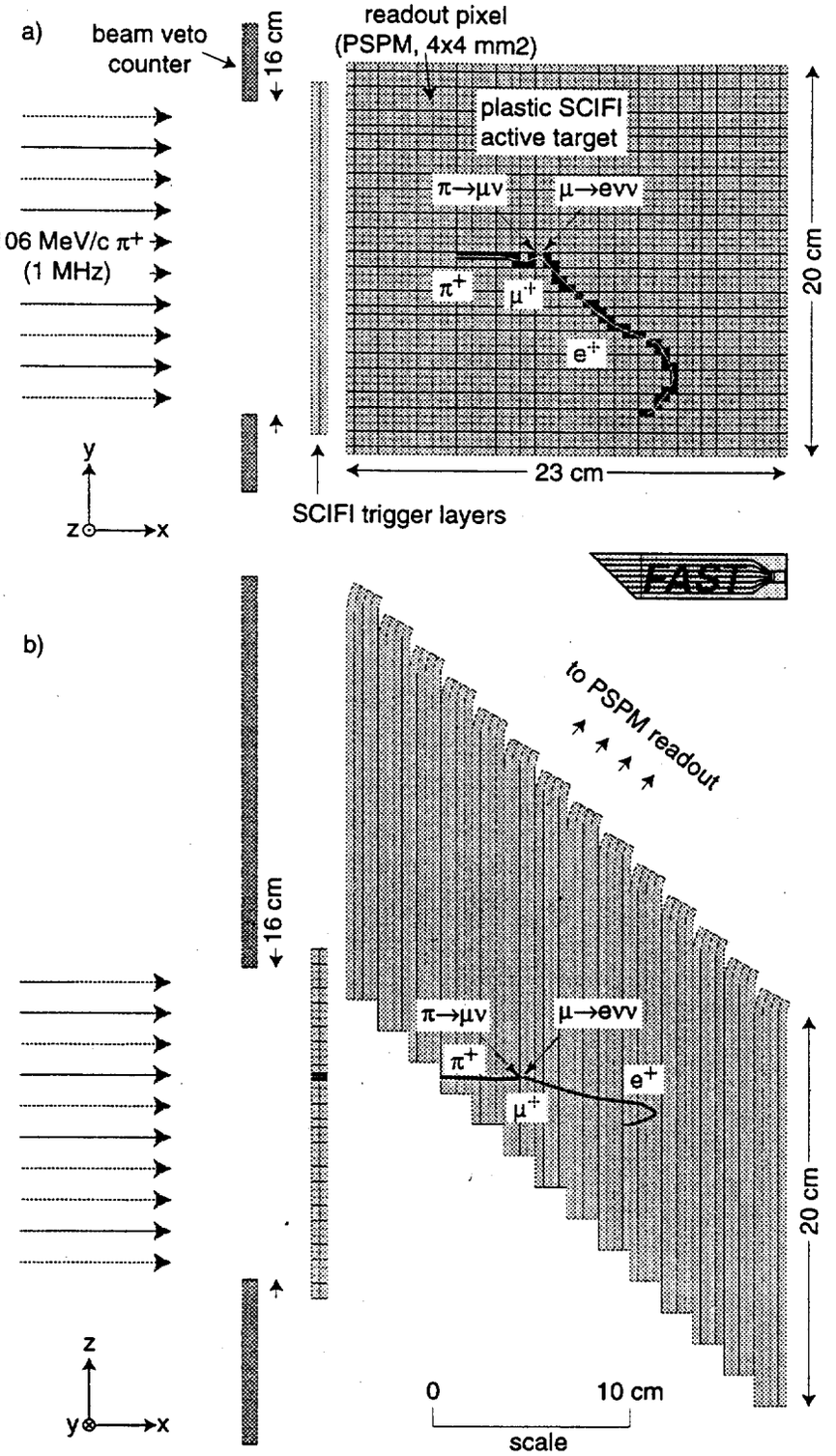

Figure 2: Option II for the FAST detector with a "card deck" geometry: a) xy projection and b) xz projection. The stopping points of the beam are spread over an area of about 16×16 cm^2 in the xy projection by the effects of straggling and by spreading or sweeping the beam transversely.

2.2 Scintillating fibre target and opto-electronic readout

The target is constructed from a parallel assembly of 0.5 mm diameter plastic scintillating fibres and has an active volume[4] of $20\times20\times20$ cm^3. It is preceded by an 8 mm-thick SCIFI trigger counter, with the fibres oriented perpendicular to those in the target. This provides the z entry coordinate of the incoming beam particle and it also reduces the possibility of a second particle entering the target simultaneously and remaining unobserved. The fibres are read out from only one side; the other fibre end face is polished and partially silvered to increase the light yield. The total fibre length required for the target and fan-out is about 50 km.

Outside the active volume, the fibres are arranged in bundles that match the dimensions of the PSPM pixels. Adjacent bundles are fed to pixels on different PSPM's in order to avoid cross-talk between neighbouring pixels, caused by the spreading of light in the space between the fibre end face and the photocathode. One candidate PSPM is the Hamamatsu R5900-M16 which has 4×4 individual anodes (pixels), each of size 4×4 mm^2 (Fig. 3). This tube has metal channel dynodes powered by a built-in divider chain, providing a high gain of up to 3×10^6. The output pulses are narrow, with a FWHM of 1.5 ns. The PSPM is very compact: the outer dimensions of the glass envelope are only $3 \times 3 \times 4.5$ cm^3. A total of 144 PSPM's (2300 pixels) is required for the full detector. The expected performance of the SCIFI/PSPM target assembly is summarised in Table 2 [11], based on measurements with Kurary SCSF-81 multiclad fibres.

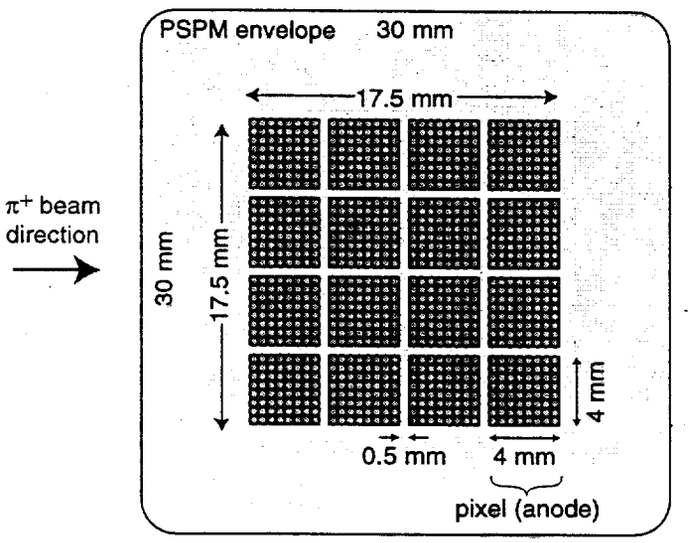

Figure 3: Geometry of the Hamamatsu R5900-M16 phototube (4×4 anodes) with scintillating fibres of 0.5 mm diameter. The pixel size (4×4 mm^2) defines the readout granularity of the detector.

A calibration and monitoring system verifies the stability of the time measurement and constantly checks proper functioning of the trigger logic. For this purpose, the partially-

[4] For clarity, the figures presented in the remainder of this document refer only to the block geometry (Fig. 1), unless otherwise indicated. The card-deck geometry (Fig. 2) requires about 15% more readout channels.

Table 2: Summary of the physics processes and their approximate signals in the detector (assuming tracks crossing perpendicular to the fibre axes).

Process	Relative time, t (ns)	Path length (cm)	#pixels /track	#p.e. /pixel	σ_t /pixel (ns)
1. π^+/μ^+ beam particle	0	2–18	5–45	35–260	$\lesssim$0.3
2. $\pi^+ \rightarrow \mu^+\nu_\mu$ decay	26 (τ)	0.15	$\sim$1	120	0.2
3. $\mu^+ \rightarrow e^+\nu_e\bar{\nu}_\mu$ decay	2200 (τ)*	$\gtrsim$2	$\gtrsim$5	25	0.4

* Decays are accepted up to 9 τ_μ, i.e. t = 20 μs.

silvered end face of the target is periodically illuminated by a light-distribution system. The light source, probably a laser, is pulsed by a rubidium clock duplicating the primary clock system of the TDC system (Section 2.4). Suitable patterns for the trigger test are generated using programmable masks.

2.3 First and second level triggers

The detection volume of FAST (48 × 48 pixels) is divided into two parts. The front two layers of the target are dedicated to first level triggering. The rest of the volume is used in second level triggering and for time measurements. Light from scintillating fibre bundles is detected by PSPM's and fed to discriminators. The time jitter of the output signals is small, even for fixed-threshold discriminators, due to the large signal pulses (Table 2).

The beam trigger and veto counters preceding the target are used to signal the entry of a single beam particle inside the fiducial volume. The first level trigger detects a coincidence of signals in the two front layers and delivers the y entry point of the beam particle to the second level trigger.The pixels of the main volume of the target are logically arranged in rows for the triggering and time measurements. All pixels of each row are processed by an associated bitmap unit.

In the remainder of this section we describe a triggering scheme for operating FAST in a DC π^+ beam. The trigger system is designed to find the stopping point of the π^+ and to check whether the event is clean or spoilt by other pions during a pre-defined period of 20 μs, equal to 9 τ_μ.

The trigger takes two snapshots of the event. The exposure of the first snapshot starts at the entrance time t_0 of the π^+ into the detector and covers the period until it stops (t_0 + 10 ns). This first snapshot provides a graphical representation of the pion track.

The exposure of the second snapshot starts as soon as possible after the π^+ stops (t_0 + 10 ns) and covers the period until it has decayed (t_0 + 240 ns, equal to 9 τ_π). The second snapshot contains the hit(s) of the secondary μ^+ and, in a small fraction of the events, it samples hits from the daughter e^+ as well. The trigger system recognises the event as a decay of a π^+ if the end of the track in the first snapshot coincides in xy space with the beginning of a secondary track in the second snapshot. Here, a spatial coincidence implies the same pixel or one immediately adjacent.

The coincidence point is taken as the stopping point of the pion. The trigger system checks whether the muon is superimposed with any other pion arriving in the time interval, $t_0 \pm 20$ μs and having a stopping point within a "super-pixel" region of 5×5 pixels around the muon. If no overlap occurs, the trigger is fired and the TDC's are read out within a small window around the muon and up to a maximum time of $t_0 + 20$ μs. If an overlap occurs, both pions are rejected. At 1 MHz beam rate the super-pixel occupancy is about 60%. We are investigating the possibility of reducing the beam overlap rate by de-randomising the stopping points in the target (Section 3).

Finally, in order to monitor the correct functioning of the trigger electronics, a pre-scaled rate of untriggered events is recorded in parallel with normal data taking. A detailed description of the trigger scheme and data acquisition system can be found in reference [12].

2.4 Time measurement

The experiment requires a high performance TDC system. Each TDC module is associated with a row (in x) of pixels in the target and measures the times of the pixel signals of this row. A TDC based on the custom chip developed for the LHC detectors by the CERN/ECP-MIC group [13] appears to be well matched to the FAST requirements. This chip is a 32-channel multi-hit TDC with zero conversion time. With a 60 MHz clock the bin size is 0.52 ns. The full scale time range is 0.55 ms (21-bit), followed by a seamless wrap-around. The chip has an internal circular hit-buffer which allows readout of all data between $t_0 - 20$ and $t_0 + 20$ μs. The two-hit resolution on a single channel is 10 ns and the rate capability is up to 1 MHz/ch, all channels driven simultaneously.

The TDC chip provides a time-stamp on each incoming hit and writes the data into the on-chip buffer memory. From here it is transferred to a FIFO memory shared by the 32 channels. For each muon, the fiducial region of interest is 5×5 pixels centred on the muon stopping point. To keep the data rate on the VME bus low, the TDC module is equipped with a skip logic that reads all hit data within the trigger time interval of each muon and stores in an event output FIFO only those hits from the muon fiducial region.

The TDC system is driven by an external 60 MHz rubidium atomic frequency standard which has a precision of better than 10^{-10} over year-long periods. This is well beyond the required precision of 10^{-7} for FAST.

2.5 Data acquisition

The DAQ system consists of 48 TDC modules, occupying three VME crates, and three SHARC-based [14] VME processor modules.

Each multi-SHARC VME processor-module of the data acquisition system receives the y coordinate of the pion stopping point from the second level trigger. For this purpose a link port (or serial port) of a SHARC processor is used. The processor module checks whether the section of the target for which it is responsible contains all event information or part of it, or if the event is displaced fully in another VME crate of the data acquisition system. In the first case the module reads the event data via its VME bus. In the second case it collects part of the data via the VME bus and sends this part to an adjacent

processing module or receives another part of the data from it. In the third case the processor module doesn't perform any action, it just skips the stopping point in question.

When a complete event is collected in the module, it is processed by the SHARC processors and the time intervals are calculated between the stopping point of the pion, the hit(s) of the muon and the initial hits of the positron. The data is accompanied by an event header, which encodes the position of the stopping point and the number of hits in the event. In total the SHARC board has to read via the VME bus 5 headers and up to 10 hits per event.

The mean rate of the output data from each processor module is below 20 Mbytes/s. The total output data rate is therefore about $3 \times 20 = 60$ Mbytes/s. This is recorded on DLT tapes for analysis and monitoring. Assuming a capacity of 200 GB per tape, the experiment would record about 1 tape per hour at 100% beam duty cycle, and the 10^{12} events would be stored on a total of about 250 tapes.

3 Accelerator requirements

In the first stage, the experiment requires a DC π^+ beam of 160 MeV/c [5] which ranges out near the down-beam end of the detector and, in the second stage, a time-structured π^+ beam of 135 MeV/c which ranges out near the centre of the detector. The DC beam intensity during the accelerator "on" time is 1 MHz.

In order to reduce the overlap probability, the beam is spread over a transverse (y) distance of about 16 cm. In addition, for the block geometry (Fig. 1), a finite beam energy spread is introduced, together with a vertical dispersion at the entrance to the target. The latter results in a spread in depth (x) of the stopping point, by a predictable amount. A wedge-shaped energy degrader located in front of the target serves to increase the spread in depth. In this way the most active pixels—those nearby or occupied by a μ^+—are spread over an area of about 16×16 cm^2 in the readout projection of the target. A second, card-deck, geometry is under investigation which avoids the need for a wedge degrader and large energy spread to distribute the x stopping points of the beam particles (see Fig. 2).

An additional approach for spreading the beam in the target is under investigation. It would reduce the overlap rate even further by *de-randomising* the beam stopping points. The technique involves continuously sweeping the beam position and/or energy to a new location in the target each $\sim$1 μs by means of electrostatic deflectors. In this way each muon stop location (super-pixel) would be visited only once approximately every 64 μs—long after any previous muon had decayed.

At present we are comparing the options for the experiment at CERN and at PSI. Some of the initial considerations are summarised below.

3.1 CERN

Compared with typical PS secondary beams, the required beam energy for FAST is lower and the required intensity higher. For example, the East Hall currently receives a 24

[5] The card-deck geometry requires a DC π^+ beam of 106 MeV/c.

GeV/c extracted beam of 4×10^{11} protons per 0.45 s pulse. In the lowest-energy beamline (T11, which is optimised for operation at 1–3 GeV/c) this provides a maximum intensity of only about 10^3 π^+ per spill at 160 MeV/c. The extracted beam intensity is limited by radiation restrictions—the PS itself could provide two orders of magnitude more beam. Assuming the radiation problems could be overcome, a new short beam line would be required (the mean flight path of a 160 MeV/c π^+ is 9 m). It would be challenging to reach a beam intensity of 1 MHz.

The PS "B cycle" is a 0.45 s spill with a minimum repetition time of 2.4 s; this would provide a maximum duty cycle of 20%. The maximum fraction of the PS beam that could be devoted to a dedicated experiment would be about half of this, i.e. 10%. Assuming a 1 MHz rate could be achieved during the spill time, the time-averaged event rate would therefore be 10^5 Hz, allowing the required sample of 10^{12} events to be recorded in about 140 days of beam time, assuming 70% detector live-time.

The PS Booster is in principle a better match to the FAST requirements. The proton momentum from the Booster is 1.7 GeV/c and it delivers 12 pulses of 3×10^{12} protons during each PS Supercycle of 14.4 s. Half of these are delivered directly to ISOLDE and the other half are injected into the PS. However only a fast extraction (2.4 μs pulse) exists at the PS Booster, and a slow extraction cannot be added. The only solution would be to build a new ring to stretch the pulses after leaving the Booster, estimated to cost several MCHF.

3.2 PSI

3.2.1 DC beam

Several suitable beam lines exist at PSI (e.g. πM1, πE1 or πE3) that can deliver beams of 1 MHz or more, the maximum being up to 1 GHz [15]. A π^+ beam momentum of 160 MeV/c is well-matched to the 590 MeV primary proton energy of the PSI cyclotron. Furthermore, the beams are delivered with 100% duty cycle, which would allow the required sample of 10^{12} events to be recorded in 14 days of beam time, assuming 70% detector live-time. This would open up the possibility of making several runs at a comparable statistical precision, but with different experimental or beam conditions, in order to control and reduce the final systematic error.

3.2.2 Time-structured beam

The proposal to construct a time-structured μ/π beam at PSI [16] provides the possibility of performing the experiment with quite different systematic errors. In this approach a short pulse of pions is injected into FAST and then the beam is switched off for the following 20 μs. This effectively creates a small "radioactive" muon source inside the detector which completely decays over this period. The time of each individual muon decay is recorded relative to a common start time for that pulse.

This beam would use a similar technique as the recently-commissioned "MORE" (muons on request) facility at PSI. To load the FAST target, an electrostatic kicker would be turned on to deliver about 20 beam particles in a 1 μs period. Then the kicker would be turned off for the next 20 μs to exclude further beam particles. The time-averaged beam rate is 1 MHz, as for the DC beam. This mode of operation is only possible at a

machine that combines high fluxes *and* high duty cycles, so that the number of muons per bunch remains reasonably small. PSI has several suitable high intensity π areas, such as πE1 or πE3, with available fluxes of 10^7–10^8 s^{-1}.

4 Systematic errors

With a 1 MHz beam rate, the proposed FAST detector and data collection system will readily reach the desired statistical precision, corresponding an event sample of 10^{12} events. The crucial problem for the lifetime measurement will be to control the systematic errors, namely to avoid any distortions of the time distribution of $\mu^+ \rightarrow e^+\nu_e\bar{\nu}_\mu$ decays at the 10^{-6} level.

Previous experiments measured the μ^+ lifetime in relatively simple detectors: G. Bardin et al. [8] used a sulphur target surrounded by a 6-fold plastic scintillator telescope in a pulsed muon beam at the Saclay accelerator. On the other hand, K.L. Giovanetti et al. [9] used a water Cerenkov target viewed by two phototubes in a DC π^+ beam at the TRIUMF accelerator. The final overall errors on the μ^+ lifetime measurements of 73 ps and 60 ps, respectively, were dominated by the statistical errors.

In the Saclay experiment [8], the largest systematic errors resulted from:

1. A rate-dependent inefficiency due to the low detector granularity, which induced an $e^{-2t/\tau}$ component in the decay time distribution. With the pulsed beam structure used in this experiment, this suppressed the detection of early muon decays relative to later ones ($\sigma_{\rm syst}$ = 27 ps).

2. Polarisation of the incoming μ^+ component of the beam followed by muon precession in the weak ambient magnetic field. Due to the limited solid angle of the detector, this resulted in an inefficiency that depended on the muon decay time ($\sigma_{\rm syst}$ = 20 ps).

3. A time dependent (beam correlated) background ($\sigma_{\rm syst}$ = 10 ps).

The TRIUMF experiment [9] used a low beam intensity (5–30 kHz) and a standard pile-up veto technique to restrict the analysis to non-overlapping events.

The FAST detector must reduce these errors by a factor of at least 30, and at event rates that are about 2 orders of magnitude larger. For operation in a DC beam, an important challenge is to avoid overlapping decays. For operation in a time-structured beam, an important requirement is to avoid any time-dependent detection inefficiencies caused by muon spin rotation. The detector addresses these and other systematic errors as follows:

- A highly granular and fast detector containing 2300 detector elements, compared with 2–6 elements in the previous experiments. This will greatly reduce the probability for two events to overlap. Overlapping events lead to a loss of events and, if undetected, introduce an $e^{-2t/\tau}$ component in the decay time distribution [16].

- For the DC π^+ beam, a positive identification of the $\pi^+ \rightarrow \mu^+\nu_\mu$ decay, which eliminates triggering by (polarized) background muons in the beam. Since the pions are unpolarized (spin 0), the decay muons produced from π^+ decays at rest

have an isotropic distribution of polarization directions. Errors from polarisation asymmetries are therefore eliminated. Earlier experiments, in contrast, could not detect the $\pi^+ \to \mu^+\nu_\mu$ decay. Although this technique for tagging each π^+ is not possible with the time-structured beam, a substantial reduction of the ($\sim$10%) muon background in the beam will be achieved by the large ($\sim$3.5 cm) difference in $\pi - \mu$ range at this momentum.

- Uniform and high detection efficiency over the full 4π solid angle. This will strongly suppress any asymmetries due to spin rotation of residual background beam muons in the time-structured π^+ beam.

- An imaging detector which strongly suppresses spurious triggers, such as accidentals from stray beam particles, neutrons or cosmic rays.

- Large pulse heights and therefore high detection efficiency over the complete e^+ energy spectrum from μ^+ decay. Positrons with energies above about 0.2 MeV (corresponding to a signal of 7 p.e.) will be detected with 100% efficiency.

- A high level of redundancy of time measurements to monitor and reduce systematic timing errors.

Simulation studies of the systematic errors are underway and the results will be included in the FAST proposal document.

5 Planning

5.1 Prototyping

A series of prototypes is required in order to develop all key parts of the FAST setup and verify their performance:

- *Target and light detection:* A first prototype of the FAST target, $200 \times 200 \times 4$ mm^3 in size and made from 0.5 mm scintillating fibres, has been provided by DESY-Zeuthen [11] and partially equipped with PSPM's at ETH Zurich. First tests using a β source produced the expected results for light output, pulse shape and cross talk. Design ideas for the coupling between fibres and PSPM were tested. In a more advanced prototype, a full section of the target will be equipped, sandwiched between solid pieces of scintillator and exposed to a pion test beam. Final data about the signal shape and light output will be collected.

- *TDC board:* The design performance and requirements of the TDC, such as the definitions of the time intervals, pixel regions and readout logic, will be tested with a 128-channel commercial board (CAEN V767) based on the CERN/ECP-MIC chip. An extensive programme of measurements, using two independent rubidium clocks, is foreseen to test the rate capability, precision and long term stability of all stages of the time measurement.

- *System tests:* First system integration tests are foreseen for November or December 1998, using the πM1 π^+ beam at PSI. Here, prototypes of all key parts of the system, including light pulsing and distribution, simplified trigger logic and time measurement electronics will be tested together in order to verify the design, interface definition and overall performance.

Results from these prototype tests will be included in the FAST proposal document.

5.2 Cost and schedule

A cost estimate for the FAST experiment is shown in Table 3. The expected timescale is for the proposal to be ready in the Spring of 1999, on completion of the prototype tests and beam tests. After approval, the experiment could be constructed in under 18 months, to start data taking by the end of 2000.

Table 3: Cost estimate.

Item	**Cost [kCHF]**
SCIFI target	100
Position-sensitive phototubes	300
Trigger electronics	150
TDC's	200
Calibration system	50
DAQ	100
Total:	**900**

6 Conclusion

Progress in particle physics requires new experiments at the frontiers of both high energy and high precision. High precision experiments such as the proposed FAST detector are able to probe fundamental aspects of the Standard Model and yet can be carried out at relatively low energies and moderate cost. This experiment will determine the Fermi coupling constant, G_F, to a precision of 10^{-6}, representing a factor of 20 improvement beyond the present world average. In combination with other fundamental parameters such as $\sin^2\theta^{lept}_{eff}$, α, m_W, m_Z and m_t, this will sharpen future precision electroweak tests of the Standard Model, and perhaps open a window to the new physics beyond.

References

[1] LEP Electroweak Working Group, *A combination of preliminary electroweak measurements and constraints on the Standard Model*, LEPEWWG/98-01 (1998).

[2] Particle Data Group, *Review of particle physics*, Phys. Rev. D54 (1996).

[3] S. Eidelman and F. Jegerlehner, *Hadronic contributions to g-2 of the leptons and to the effective fine structure constant* $\alpha(m_Z^2)$, Z. Phys. C67 (1995) 585; J. Blumlein, F. Jegerlehner and T. Riemann, *Hadronic vacuum polarization contribution to g-2 of the leptons and* $\alpha(m_Z^2)$, Nucl. Phys. B, Proc. Suppl. 51C (1996) 131.

[4] The BES collaboration at BEPC is currently making a precision measurement of $\sigma(e^+e^- \rightarrow \text{hadrons})$ in the τ-charm threshold region (Li Weiguo, private communication).

[5] J.H. Kuhn and M. Steinhauser, *A theory driven analysis of the effective QED coupling at* m_Z, MPI-PhT-98-12 (1998); M. Davier and A. Hocker, *New results on the hadronic contributions to* $\alpha(m_Z^2)$, LAL-98-38 (1998).

[6] J.H. Kuhn et al., in preparation.

[7] M.P. Balandin et al., Sov. Phys. JETP 40 (1974) 811.

[8] G. Bardin et al., *A new measurement of the positive muon lifetime*, Phys.Lett.B 137 (1984) 135.

[9] K.L. Giovanetti et al., *Mean lifetime of the positive muon*, Phys. Rev. D 29 (1984) 343.

[10] An experiment is currently under consideration to measure the μ^+ lifetime at the Brookhaven AGS to a precision comparable to this proposal: R.M. Carey et al. (Boston-Brookhaven-Illinois-Minnesota collaboration), *Letter-of-Intent for a new measurement of the* μ^+ *lifetime*, BNL (1997).

[11] E.C. Aschenauer et al., *Test results from prototype fibre detectors for high-rate particle tracking*, DESY-98-001 (1998), submitted to *Nucl. Int. Meth.*

[12] A. Menchikov and R.Nahnhauer, *A possible scheme for the trigger and data acquisition of the FAST detector*, DESY Zeuthen 98-01 (1998).

[13] J. Christensen, *An integrated high resolution CMOS timing generator based on an array of delay locked loops*, IEEE Journal of Solid-State Circuits, 31 (1996) 952; J. Christensen, *32-channel general purpose time-to-digital converter*, CERN/ECP-MIC internal note, http://pcvlsi5.cern.ch:80/MicDig/jorgen/tdc32_ma.pdf (1997).

[14] More details on the processors can be found at the Design Support web site at http://www.analog.com/support/frames/ dsp_frameset.html.

[15] PSI Users' Guide; Accelerator Facilities (1994).

[16] P. Kammel, F. Foroughi, C. Petitjean and D. Renker, *Letter-of-intent for a high intensity muon/pion beam with time structure at PSI*, PSI-R-98-04.0.